Zircon U-Pb age of tuffaceous sandstone in the southern margin of Turpan-Hami Basin and its geological significance

Tingting Fan *, Haokai Yang, Feixiang Che and Mengying Zhou

College of Geology and Environment, Xi'an University of Science and Technology, Xi'an, China

* Corresponding Author Email: fantingting@xust.edu.cn

Abstract. The Dongdagou area of Yamansu in the southeastern margin of Turpan-Hami basin, which is located to the north of the Kangguertag collision zone, is one of the representative areas to discuss whether there is a Precambrian basement problem in the Junggar Turpan-Hami massif. As a consequence, zircon LA-ICP-MS U-Pb dating has been carried out for the shallow metamorphic tuffaceous fine sandstone in the Yamansu formation of the Lower Carboniferous in this area. The results show that the ages of 30 clastic zircons range from 365 ±3 Ma to 2451 ±39 Ma, with multi-peak distribution characteristics. The ages of clastic zircons are mainly concentrated in 365~496 Ma, the main peak is 365~436Ma, the secondary peak is 440~496 Ma, and the ages of 8 clastic zircons are between 765~2451 Ma. The study shows that the formation age of the sedimentary rock is not the early Carboniferous but the late Middle Devonian. Based on the isotopic dating data of the two-cloud quartz schist in the Xiaohuangshan area in the northeast of the study area, it is considered that the lower limit of the formation period of this set of strata is not earlier than the Devonian. Combined with the age data of ancient zircons in diabase and fused tuff in the study area, and the comprehensive analysis of regional sedimentary characteristics, it is concluded that there may be Precambrian crystalline basement in the sediment source area-Junggar-Turpan-Hami block.

Keywords: Clastic zircon, Yamansu formation, basement, Turpan-Hami basin.

1. Introduction

The study on the basement properties of the Junggar-Turpan-Hami block is very important for analyzing the structural characteristics and evolution of the northern Xinjiang and Central Asian orogenic belts, and for exploring oil, gas, coal and other mineral resources in the basin. However, there are still great differences in the tectonic attribute and evolution history of the basement. The low mountain and hilly Gobi area between the southern Turpan-Hami basin and the Tarim basin is the East Tianshan orogenic belt. There are many scientific problems in the evolution of Paleozoic oceanic-continental tectonic framework and its complex orogeny in the East Tianshan region [1-5]. A set of tuff and tuff clastic rocks with a thickness of 5636.29m are developed in Dongdagou area of Yamansu town in the southeastern margin of Turpan-Hami basin. It is divided into Yamansu formation of Lower Carboniferous in the range of 1: 200000 Hongliuhe, and the research degree is weak. On the basis of detailed field geological survey, the author has studied the LA-ICP-MS zircon U-Pb dating of tuffaceous sandstone in order to re-recognize the formation age of this set of strata and provide research data for the study of basement properties of Junggar-Turpan-Hami massif.

As shown in Figure 1a, the study area was located on the southeastern margin of the Turpan-Hami basin and on the north-east side of the Kangguertage collision zone. This area is the eastern extension of the Paleozoic active continental margin belt in the southern margin of Turpan-Hami basin. The administrative division belongs to Yamansu Town, Hami City, and Xinjiang Uygur Autonomous region. The strata exposed in the area are mainly Carboniferous strata, mainly the Lower Carboniferous Yamansu formation, followed by the Lower Carboniferous Xiaorequanzi formation and the Upper Carboniferous Dikaner formation. The Yamansu formation was mainly composed of thick gray-green and grayish-brown tuff and gray and brown tuffaceous clastic rocks, with mylonitized bioclastic limestone at the top and rich fossils of corals and gastropods. The Xiaorequanzi formation was composed of gray, grayish green, reddish brown tuffaceous sandstone and grayish green and sauce red tuff. The main lithology of Dikaner formation was gray-black, gray-green tuff, tuffaceous sandstone intercalated with gray-black siliceous rock and siliceous mudstone, and the bottom was a thick layer of dark gray pillow basalt.

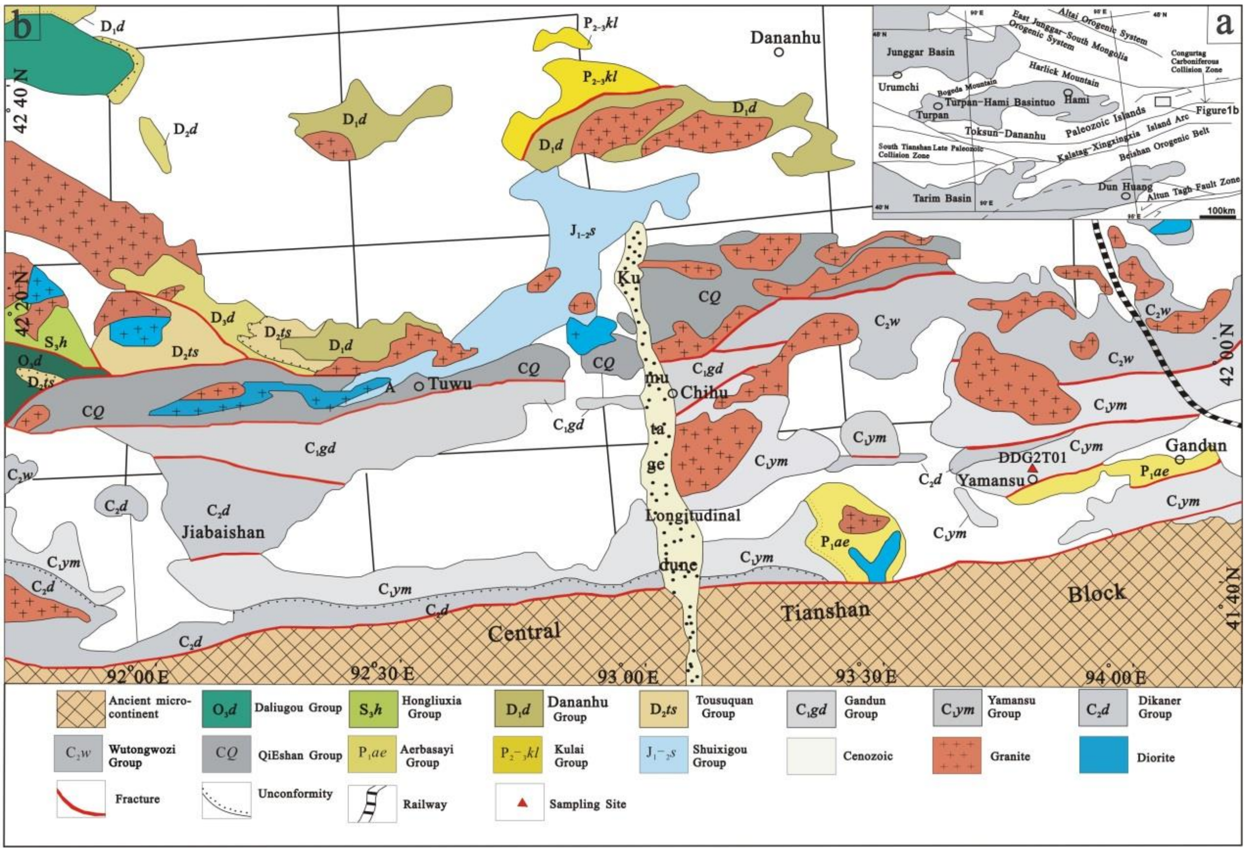

Figure 1. Geological sketch map of the southern Turpan-Hami Basin (modified after [6]).

2. Sampling position and sample characteristics

The DDG2T01 samples of metamorphic tuffaceous fine sandstone were collected from the south of Dongdagou, Yamansu Town, Hami City (Figure 1b), with coordinates of 94°00′48.5″E and 41°58′02″N In the field outcrop, the rock assemblages were mainly as follows: the upper part of the sampling site was composed of reddish brown, gray-green tuffaceous coarse sandstone, fine sandstone and siltstone, and the middle part was brown tuffaceous coarse sandstone, fine sandstone and tuff with a small amount of gray-green tuffaceous coarse sandstone, quartz veins were developed, and DDG2T01 samples were collected in brown tuffaceous fine sandstone. The lower part was gray, reddish brown coarse sandstone, tuffaceous sandstone and tuff. The study horizon belonged to the lower subgroup C_1y^a, of the Yamansu formation of the Lower Carboniferous, which was in contact with the C_1y^b fault of the upper subgroup of the Yamansu formation of the overlying strata.

As shown in Figure 2 under the microscope, the detritus in tuffaceous fine sandstone was mainly feldspar (with an average content of about 45 %), quartz (with an average content of about 35 %), tuffaceous cuttings (with an average content of about 15 %) and extrusive cuttings (with an average content of about 5 %). The detritus grain size was generally 0.1~0.25 mm. Feldspar had a strong sericitization. The cement content was 20 %, which was mainly tuff and its alteration products with strong chlorite, Ili petrification and pyrite generally occur. Under the microscope, it could be seen that pyrite was scattered and disseminated.

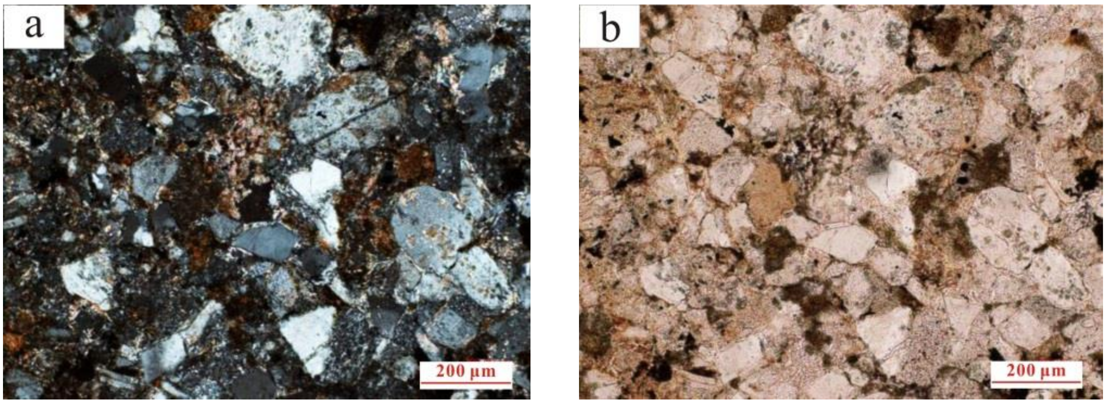

Figure 2. DDG2T01 micrograph of tuffaceous sandstone, a. Orthogonal polarization; b. Single polarized light

3. Zircon characteristics and test results

Zircon separation was completed in Hebei Langfang Institute of Mineral Geological Survey. Sample preparation, reflected light, cathodoluminescence and U-Pb isotope analysis were completed in the State key Laboratory of Continental Dynamics, Northwestern University. The instrument used in the experiment was Agilent 7500a, and the spot of the laser beam was 30 μm. The laser denudation system was GeoLas200M and the wavelength was 193nm. Test and data processing were carried out according to the standard determination procedure [7]. $^{207}Pb/^{206}Pb$ surface age was used for zircon ages over 10Ga and $^{206}Pb/^{238}U$ surface age for zircons less than 10Ga [8].

30 points of 29 zircons in metamorphic tuffaceous fine sandstone DDG2T01 samples were dated by ICP-MS U-Pb, and 28 harmonic ages with a harmony degree of 90% to 110% were obtained. From the zircon CL image of tuffaceous sandstone in Figure 3, it can be seen that the zoning structure of zircon was relatively clear. Table 1 showed the calculated results of U/Pb isotopic composition and surface age in the sample, in which the isotope ratio and the age error of a single point are both 1 δ. The contents of U and Th were 85.16×10^{-6} ~ 511.16×10^{-6} and 44.19×10^{-6} ~ 326.78×10^{-6}, respectively. The Th/U ratios were all greater than 0.1and only 4 were less than 0.4. The cathodoluminescence characteristics and Th/U ratios show ED that most of these clastic zircons belong to magmatic zircons and some of them were affected by metamorphism.

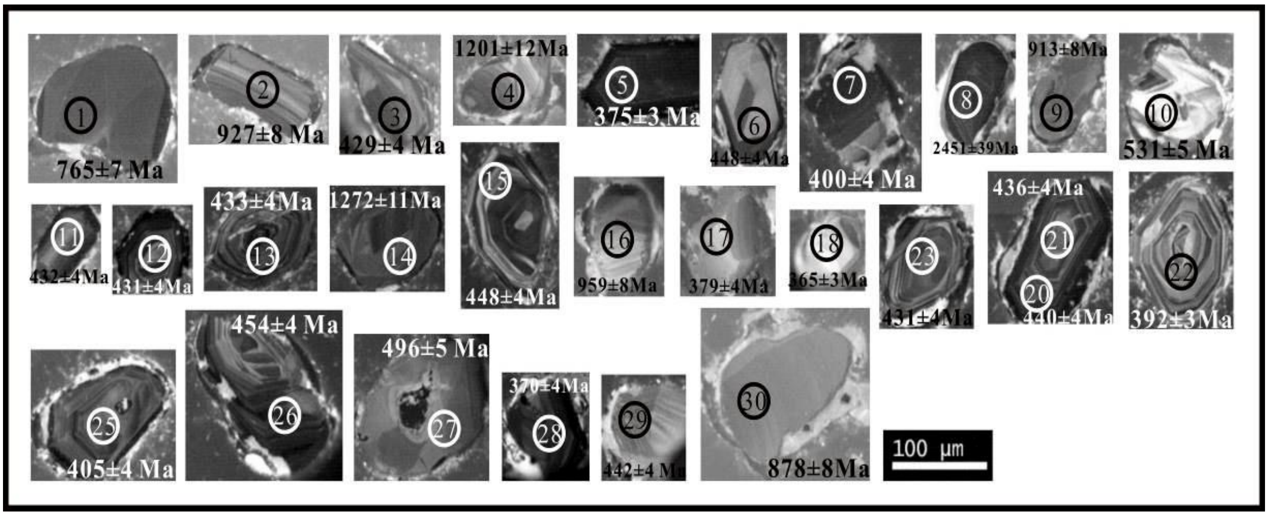

Figure 3. Cathodoluminescence image of tuffaceous fine sandstone DDG2T01 zircon.

According to the analysis data in Table 1, the U-Pb surface age values of DDG2T01 zircons in tuffaceous sandstone range from 365 ±3 Ma (point 18) to 2451 ±39Ma (point 8). All the points of the zircon $^{207}Pb/^{235}U$ - $^{206}Pb/^{238}U$ harmonic diagram (Figure 4b) fall on or near the harmonic line, showing good harmony, and there is no obvious lead loss.

Table 1. Results of DDG2T01 zircon LA-ICP-MS U-Pb isotopic chronological analysis of tuffaceous sandstone in eastern Yamansu.

Samples	element contents ($\times 10^{-6}$) and ratios				isotope ratio				Age (Ma)							
	^{206}Pb	^{232}Th	^{238}U	Th/U	$^{207}Pb/^{206}Pb$	± (%)	$^{206}Pb/^{238}U$	± (%)	$^{207}Pb/^{206}Pb$	1δ	$^{207}Pb/^{235}U$	1δ	$^{206}Pb/^{238}U$	1δ	$^{208}Pb/^{232}Th$	1δ
DDG2T01-1	311	145	355	0.41	0.06535	0.00183	0.12600	0.00122	786	60	770	14	765	7	764	7
DDG2T01-2	144	141	216	0.65	0.06860	0.00153	0.15467	0.00144	887	14	915	8	927	8	1031	11
DDG2T01-3	79	117	246	0.47	0.05641	0.00133	0.06875	0.00064	469	18	435	5	429	4	462	5
DDG2T01-4	99	80	108	0.74	0.08017	0.00177	0.20275	0.00191	1201	12	1194	9	1190	10	1160	11
DDG2T01-5	103	226	363	0.62	0.05752	0.00134	0.05988	0.00055	512	17	395	5	375	3	422	5
DDG2T01-6	54	136	158	0.86	0.06231	0.00153	0.07200	0.00069	685	20	489	6	448	4	487	5
DDG2T01-7	71	141	200	0.70	0.05534	0.00154	0.06406	0.00064	426	29	404	7	400	4	438	5
DDG2T01-8	358	202	172	1.17	0.15960	0.00359	0.46453	0.00493	2451	39	2455	18	2460	22	2461	24
DDG2T01-9	249	80	362	0.22	0.07658	0.00128	0.15209	0.00138	1110	34	973	9	913	8	903	8
DDG2T01-10	41	236	92	2.55	0.06382	0.00189	0.08585	0.00092	736	31	571	10	531	5	549	6
DDG2T01-11	90	173	275	0.63	0.05795	0.00138	0.06925	0.00065	528	19	447	6	432	4	477	5
DDG2T01-12	74	140	227	0.62	0.05915	0.00147	0.06907	0.00066	573	21	454	6	431	4	473	6
DDG2T01-13	96	184	289	0.64	0.06451	0.00146	0.06953	0.00064	758	15	489	5	433	4	492	5
DDG2T01-14	123	44	139	0.32	0.08312	0.00177	0.18661	0.00171	1272	11	1162	8	1103	9	1098	12
DDG2T01-15	73	145	214	0.68	0.05731	0.00137	0.07189	0.00067	503	19	457	6	448	4	492	5
DDG2T01-16	171	64	227	0.28	0.07087	0.00151	0.16047	0.00146	954	11	958	7	959	8	1054	12
DDG2T01-17	59	99	185	0.54	0.05669	0.00160	0.06057	0.00062	479	30	394	7	379	4	403	6

DDG2T01-18	113	327	385	0.85	0.05913	0.00136	0.05823	0.00054	572	16	395	5	365	3	385	4
DDG2T01-20	52	88	152	0.58	0.05878	0.00147	0.07067	0.00068	559	22	460	6	440	4	504	6
DDG2T01-21	52	99	153	0.65	0.05881	0.00154	0.07003	0.00069	560	25	457	7	436	4	487	6
DDG2T01-22	165	324	511	0.63	0.05898	0.00126	0.06268	0.00056	566	13	418	4	392	3	422	4
DDG2T01-23	87	90	263	0.34	0.05505	0.00123	0.06920	0.00063	414	15	429	5	431	4	481	5
DDG2T01-25	52	88	152	0.58	0.05712	0.00137	0.06483	0.00061	496	19	419	5	405	4	457	5
DDG2T01-26	118	249	354	0.70	0.06205	0.00163	0.07291	0.00073	676	24	492	8	454	4	531	7
DDG2T01-27	51	85	140	0.61	0.06061	0.00158	0.07994	0.00079	625	24	520	8	496	5	572	7
DDG2T01-28	47	72	132	0.54	0.05584	0.00151	0.05915	0.00059	446	27	381	6	370	4	417	6
DDG2T01-29	29	51	101	0.50	0.05616	0.00128	0.07091	0.00065	459	17	444	5	442	4	469	5
DDG2T01-30	82	188	249	0.75	0.07334	0.00176	0.14594	0.00144	1023	17	921	10	878	8	1029	10

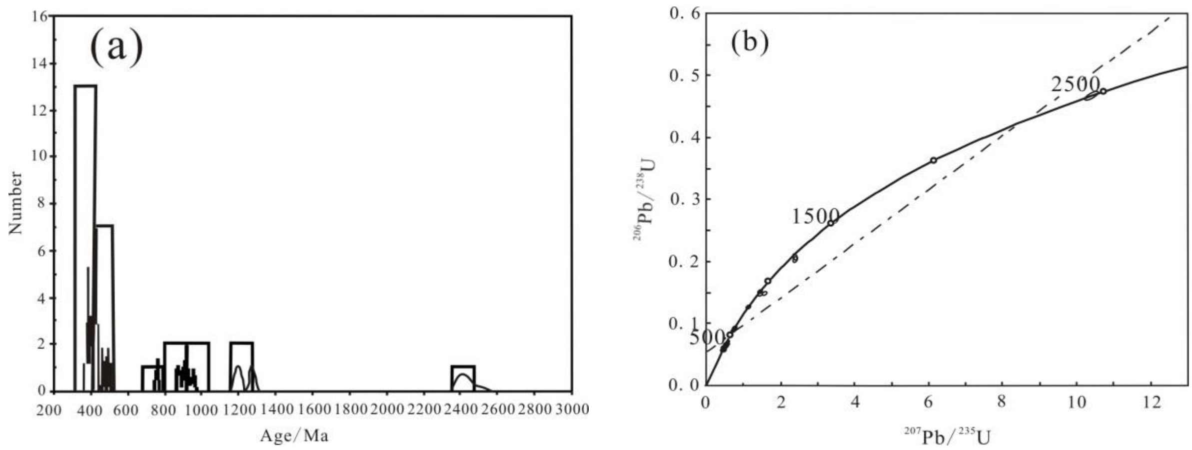

Figure 4. DDG2T01 zircon age distribution histogram of tuffaceous sandstone (a) and zircon $^{207}Pb/^{235}U$ - $^{206}Pb/^{238}U$ harmonic diagram (b).

According to the CL characteristics (Figure 3) and age distribution (Figure 4) of clastic zircons in tuffaceous sandstones, the U-Pb ages of clastic zircons studied can be divided into the following age groups: (1) 365~436 Ma: 13 zircons (point 3, 5, 7, etc in Figure 3.), the $^{232}Th/^{238}U$ ratio is between

0.34 and 0.85. Some of the zircons (point 22, 25, 12, 23, 13, and 21 in Figure 3) have obvious magmatic rhythmic zones. Only one Th/U ratio is 0.34, and the rest are magmatic zircons with more than 0.4. Zircons are semi-self-shaped columnar and well-rounded, and some of them (point 22, 25, 12, 23, 13, 21) have obvious magmatic rhythmic zones. There are also a small number of zircons (7, 11, 17, and 18 in Figure 3) whose zoning is unclear and may have suffered metamorphism. (2) 440~496 Ma: 6 zircons (point 6, 15, 20, etc.in Figure 3), the $^{232}Th/^{238}U$ ratio is between 0.54 and 0.86, the zircon oscillatory zone is not clear in the CL image, and some zircons (point 6, 26, 27 in Figure 3) may be affected by metamorphic events. (3) 531 Ma: 1 zircons (point 10 in Figure 3), the $^{232}Th/^{238}U$ ratio is 2.56. The magmatic prosodic zoning of zircons is unclear, the luminescence is not uniform, and dark accretion edges are seen on the edges, which may have undergone secondary transformation. (4) 765~959 Ma: 5 zircons (point 1, 2, 9, 16, and 30 in Figure 3). The $^{232}Th/^{238}U$ ratio is between 0.22-1.34, and the zircon CL shows that the zircon grains are highly rounded, and the internal structure of zircon is zoning-free or weak zoning structure, indicating that they may have been transported for a long distance and affected by metamorphism. (5) 1201 Ma and 1272Ma: 2 zircons (point 4 and 14 in Figure 3), $^{232}Th/^{238}U$ ratios are 0.32 and 0.74, respectively. There are obvious zoning, and thin white or dark accretive edges can be seen on the edge of zircon, indicating that it may be disturbed by hydrothermal activity. (6) 2451 Ma: 1 zircon (point 8 in Figure 3). The $^{232}Th/^{238}U$ ratio was 1.17. It should be magmatic zircon because of its good grinding, unclear banding and dark glow.

4. Discussion

The internal structure and U/Pb isotopic composition of zircons reflected by zircon cathodoluminesc-entce images of tuffaceous sandstone DDG2T01 samples showed that most zircons had the characteristics of typical magmatic zircons. The high degree of grinding at the edge indicated that it may also be affected by melting after long-distance transportation, resulting in the appearance of prism and harbor-like structure on the edge of zircon. A few zircons have complex internal structures, and there is little difference in core-mantle luminescence characteristics. The edges of some zircons are characterized by very narrow but bright CL images (point 1, 2, 25, 26, etc in Figure 3.) may be caused by late thermal events or the formation of retrograde metamorphism in the later stage of metamorphism.

The zircons of different ages vary greatly in the samples, with the largest number of zircons from Silurian and Proterozoic. Each accounts for 28.57 % of the total, followed by 7 Devonian with a content of 25 %; 3 Ordovician with a content of 10.71 %, and 2 Cambrian with a content of 7.14%. The age distribution of clastic zircons has a wide time span, indicating the complexity and diversity of the provenance composition of tuffaceous clastic rocks in Dongdagou, Yamansu Town, and Hami City, which is used for LA-ICP-MS zircon U-Pb dating. The average age of the youngest seven magmatic zircons in tuffaceous sandstone DDG2T01 clastic zircons is 384 ±4Ma, which limits the upper limit of sedimentary age of the sample, indicating that the tuffaceous sandstone is more likely to be formed in the late Middle Devonian than during the early Carboniferous. In addition, the youngest nine clastic zircons obtained from the XHST01 of the lower Carboniferous Yamansu formation quartz schist (original sandstone) in the Xiaohuangshan area in the northeastern part of the study area have a peak age of 360~412 Ma, with an average age of 379 ±5 Ma, limiting that the lower limit of the sedimentary period of the rock is not older than that of the late Devonian. It is inferred that the stratigraphic age of the Lower Carboniferous Yamansu formation in the 1: 200000 Hongliuhe amplitude of the southern Turpan-Hami basin may be Devonian.

Besides, there are 8 clastic zircons in DDG2T01 samples of tuffaceous sandstone with ages between 765 ± 7 Ma ~ 2451 ± 39 Ma, representing the zircon formation age of rocks in the sediment source area. A total of 23 age data (published in another paper) have been obtained from the XHST01 of the two-cloud quartz schist (original sandstone) in the Xiaohuangshan area, representing the provenance of the Mesoproterozoic-late Proterozoic tectonic-thermal event. According to the zircon dating data of Triassic diabase YDA01 and fused tuff YDA02 in Dongdagou, Yamansu, seven zircon ages are between 586 ± 5 Ma ~2407 ± 27 Ma (published in another article). These ancient age peaks are partially consistent. It shows that the zircon formation age of both the sediment source rock and the surrounding rock of the magmatic ascending spillway is older than that of the Cambrian.

Paleozoic oceanic crust fragments can be seen on the periphery of the Junggar-Turpan-Hami massif since the Junggar-Turpan-Hami massif had an alternating oceanic-continental pattern from the late Neoproterozoic to the Carboniferous [9]. The closure of the paleo-oceanic basin before the Karamaili ophiolitic melange belt in the northeast of Junggar Basin occurred in the late Carboniferous [10]. The oceanic basin represented by Bayingou ophiolite in the Dongtian Mountain closed in the early Carboniferous [11]. The oceanic basin represented by the western Junggar ophiolite and the oceanic crust fragments in the East Tianshan Kangguertag fault zone closed in the early Carboniferous[9]. Therefore, the ocean basins around the Yamansu Dongdagou and Xiaohuangshan areas in the south of the Turpan-Hami basin were not closed during the deposition of clastic rocks in the early Devonian, so their ancient clastic materials could not come from the Altai ancient crystalline basement in northern Xinjiang. Nor can it come from the Tarim plate, Kazakh plate and Siberia plate in the neighboring region. It can only come from the Junggar-Turpan-Hami block itself to the north of Tianshan, which is surrounded by Paleozoic oceanic basins. Therefore, it is concluded that these Precambrian age data reflect that there may be ancient crystalline basement in the sediment source area and magmatic ascending overflow area. This is also consistent with Li Yaping's understanding of 22 553~3073 Ma ancient zircons and their significance in the study of clastic zircons from the original Devonian Karamaili formation sandstones south of the Karamaili fault [9]. In addition, in recent years, there are a large number of Precambrian clastic zircons in the Paleozoic sedimentary rocks in some areas of Junggar or Precambrian gneiss capture bodies in intrusive rocks, which provide evidence for the existence of Archean crystalline basement in Junggar [12-16].

The Lower Carboniferous Yamansu formation in Dongdagou area of Yamansu is a set of sedimentary strata interbedded by tuff and tuffaceous clastic rock, interbedded with Jasper and thin siliceous rock according to field investigation and profile measurement. In addition, the top is bioclastic limestone with a thickness of about 89 m. It is rich in gastropod, coral and sea lily stem fossils. It represents a continental shelf-slope facies environment with deeper water body. The above geological practice of the Lower Carboniferous sedimentary rock series and sedimentary-volcanic rock series in the study area shows that the corresponding sedimentary environment and sedimentary provenance need to be based on the continental crust basement. It was believed that there was a continental crust basement in the Junggar-Turpan-Hami block in the Paleozoic. According to the pre-Mesozoic regional tectonic framework extending in the east-west direction, it is inferred that the continental crust basement of eastern Junggar should be extended under the Junggar basin, which remains to be confirmed by further study.

5. Conclusion

Zircon U-Pb dating is carried out on the tuffaceous fine sandstone of the Lower Carboniferous Yamansu formation in Dongdagou area of Yamansu, Turpan-Hami Basin. It is considered that the main body of the Lower Carboniferous Yamansu formation was formed in the Devonian according to the latest average age data of clastic zircons 384 Ma and the youngest group of zircons of the two-dolomite schist in the Xiaohuangshan area.

The Lower Carboniferous Yamansu formation in Dongdagou area of Yamansu is exposed to the north of Dongtian Mountains. The 765~2451 Ma zircons of tuffaceous fine sandstone are derived from the Junggar-Turpan-Hami massif, which provides favorable evidence for the existence of Precambrian crystalline basement in Junggar.

Acknowledgments

This work was financially supported by National Natural Science Foundation of China (41641018) fund.

References

[1] M.B. Allen, B.F. Windly and Zhang C, Paleozoic collisional tectonics and magmatism of the Chinese Tien Shan, central Asia, Tectonophysics. 220 (1992) 89-115.

[2] Gao J, Li M S, Xiao X C, Tang Y Q and He G Q, Paleozoic tectonic evolution of the Tianshan Orogen, northwestern China, Tectonophysics. 287 (1998) 213-231.

[3] Xiao W J, Zhang L C, Qin K Z, Sun S and Li J L, Paleozoic accretionary and collisional tectonics of the eastern Tianshan(China):Implications for the continental growth of Central Asia, American Journal of Science. 304 (2004) 370-395.

[4] Xiao W J, B.F. Windley, Huang B C, Han C M, Yuan C, Chen H L, Sun M, Sun S and Li J L, End Permian to Mid-Triassic termination of the southern Central Asian Orogenic Belt, International Journal of Earth Sciences. 98 (2009) 1189-1217.

[5] Wang G C, Shen T Y, Chen C, Ji J L, Wang A, Basin-Range Coupling and Tectonic Topography Analysis during Geological Mapping on Covered Area: A Case Study of Turpan-Hami Basin, Eastern Tianshan, Earth Science. 45(2020) 4313-4331.

[6] Bai J K, Liu C Y, Zhang S H, Lu J C and Sun J M, Zircon U-Pb geochronology and geochemistry of basalts from theQi'eshan Group in the southern Turpan-Hami Basin, East Tianshan: Constraints on closure time of the North Tianshan Ocean, Acta Petrologica Sinica. 34 (2018) 2995-3010.

[7] YUAN H L, WU F Y, GAO S, LIU X M, XU P , SUN D Y, Determination of U-Pb age and rare earth element concentrations of zircons from Cenozoic intrusionsin northeastern China by laser ablation ICP-MS, Chinese Science Bulletin. 48 (2003) 2411-2421.

[8] K.N. Sircombe, Tracing provenance through the isotope ages of littoral and sedimentary Detrital Zircons, eastern Australia, and Sedimentary Geology. 124 (2001) 47-67.

[9] LI Y P, LI J Y, SUN G H, ZHU Z X, YANG Z Q, Basement of Junggar basin: evidence from detrital zircons in sandstone of previous Devonian Kalamaili formation, Acta Petrologica Sinica. 23 (2007) 1577-1590.

[10] LI J Y, YANG T N, LI Y P, ZHU Z X, Geological features of the Karamaili faulting belt, eastern Junggar region, Xinjiang, China and its constraints on the reconstruction of Late Paleozoic ocean-continental framework of the Central Asian region, Geological Bulletin of China. 28 (2009) 1817-1826.

[11] XU X Y, XIA L Q, MA Z P, LI X M, XIA Z C, WANG L S, Accurate dating of Bayingou ophiolite in northern Tianshan Mountains and its tectonic significance, Journal of Earth Science and Environmental. 27 (2005) 17-20.

[12] CHEN D C, ZHAO X M, DENG J. U-Pb Dating of Carboniferous Sandstone Detrital Zircon from the North of the Bogda Mountains, Eastern Xinjiang, and Its Geological Significances, Acta Geologica Sinica. 84 (2010) 1770-1780.

[13] LONG X P, YUAN C, SUN M, Geochemistry and U-Pb detrital zircon dating of Paleozoic graywackes in East Junggar, NW China: insights into subduction-accretion processes in the southern Central Asian Orogenic Belt, GondwanaResearch. 21 (2012) 637-653.

[14] XU X W, LI X H, JIANG N, Basement nature and origin of the Junggar terrane: New zircon U-Pb-Hf isotope evidence from Paleozoic rocks and their enclaves, Gondwana Research. 28 (2015) 288-310.

[15] FAN T T, LIU Y Q, ZHAO W B, BAI Q H, Zircon U-Pb dating for the tuffaceous sandstone from drilling well of central Junggar Basin and its geological implications, Journal of Northwest University (Natural Science Edition). 47 (2017) 568-576.

[16] BAI J K, CHEN J L, TANG Z, LU J C, SUN J M, The closure time of Junggar Paleozoic oceanic basin: Evidence from Carboniferous detrital zircon U-Pb geochronology in Kalamaili area, Geological Bulletin of China. 37 (2018) 26-38.